Noise processes in InAs/Ga(In)Sb Corbino structures

Loah A. Stevens, ¹ Tingxin Li², Rui-Rui Du, ^{1,3} and Douglas Natelson ^{1,4.5*}

¹Department of Physics and Astronomy, Rice University, Houston, TX 77005, USA

²Department of Applied and Engineering Physics, Cornell University, Ithaca, NY 14853, USA

³International Center for Quantum Materials, Peking University, Beijing 100871, China

⁴Department of Electrical and Computer Engineering, Rice University, Houston, TX 77005, USA

⁵Department of Materials Science and NanoEngineering, Rice University, Houston, TX 77005, USA

Two-dimensional topological insulators are of great interest, with predicted topological protection

of one-dimensional helical edge states at their boundaries. Shot noise, the fluctuations in driven

current due to the discreteness of charge carriers, has been proposed as a way of distinguishing

between trivial and nontrivial edge state conduction, as well as a means of assessing back-

scattering mechanisms in the latter. Such measurements require an understanding of possible

contributions to the noise from contacts and conduction in the 2D bulk. We present noise

measurements in Corbino structures based on InAs/Ga(In)Sb quantum well interfaces over a broad

temperature and applied current range. As the temperature is lowered and the bulk transport is

gapped out, shot noise becomes detectable in these two-terminal devices, in both high- and low-

frequency measurement techniques. Quantitative comparison with a noise model shows that the

total applied voltage drop is split among the contacts and the bulk, and that the devices have some

intrinsic asymmetry. Within that model, the magnitude of the shot noise appears to be anomalously

large, implying the contacts to the 2D bulk are nontrivial in this system.

Two-dimensional topological insulators (2DTIs) with topological number Z_2 are theorized

to exhibit time reversal symmetry protected quantum spin Hall effect (QSHE).¹⁻⁴ The first

* natelson@rice.edu

1

experimental evidence was in a HgTe/CdTe quantum well (QW)⁵ where quantized edge conduction matched theoretical predictions, an observation later also made in InAs/GaSb and InAs/GaInSb QWs.^{6–8} Semiconductor QWs continue to be at the forefront of QSHE studies. In InAs/GaSb QWs specifically, wavefunction hybridization of the electron and hole bands results in a gap opening in the 2D bulk.⁹ Along the device edges, however, a Kramers pair of spin-momentum-locked 1D states persist.¹⁰ Signatures of these edge states have been observed experimentally for several years.^{6,7,11–18}

In an InAs/GaSb bilayer, the ground electron subband of InAs crosses with the ground hole subband at wavevectors k_{cross} . At k_{cross} , spatially-separated electrons and holes are strongly coupled due to tunneling between the QWs, opening the hybridization gap Δ at the crossing point in the bulk. Previous studies attempted optimization of band inversion by varying QW widths and gate voltages, $^{6,7,9,11-16,18}$ resulting in a great range of transport properties of the bulk. Most recently, Du *et al.* found by using strained-layer InAs/GaInSb, the QWs can be narrowed, resulting in larger overlap between the electron and hole wavefunctions. The InAs/Ga_{0.68}In_{0.32}Sb QWs used for this study exhibited a hybridization gap of ~20 meV, extracted from the activation energy of the bulk conduction, and the observed temperature dependence of the device resistances is quantitatively consistent with the sheet resistances of Figure 2g of Reference 8.

Several models of current noise in quantum spin Hall insulators suggest shot noise can be used to indicate the presence of nontrivial edge states or to identify back-scattering mechanisms affecting the helical edges.^{19–27} To fully understand experimental measurements, however, it is beneficial to know how contacts and the bulk may contribute to shot noise. We have performed noise spectroscopy measurements on Corbino disk structures of InAs/Ga_{0.68}In_{0.32}Sb to focus on shot noise behavior of the 2D bulk and contacts.

Shot noise arises due to the discrete nature of charge carriers; though there is some average current, individual arrival events of electrons from source to drain vary in time. For a two-terminal device, we expect the total current noise spectral density (A^2/Hz) to be given by²⁸

$$S_I = F \times 2eI \coth(eV/2k_BT) + (1 - F) \times 4k_BTG$$
 (1)

where I and V are the current and voltage bias across the junction, G is the two-terminal conductance, and F is the Fano factor, a measure of how the high bias $(eV \gg 2k_BT)$ shot noise compares to the ideal Poissonian value $S_I = 2eI$. Equation 1 is a phenomenological expression designed to give the correct Johnson-Nyquist noise $(4k_BTG)$ at I,V=0 and a bias-independent Fano factor in the limit $eV \gg 2k_BT$. Both shot noise and Johnson-Nyquist noise are expected to be white over the frequency ranges of interest.

Shot noise is generally not measurable in macroscopic conductors. As the length of a diffusive conductor increases beyond the inelastic mean free path for scattering energy out of the charge carriers, strong electron-phonon interactions cause shot noise to decay with increasing length until it is fully suppressed when the electrons have thermalized to the phonon temperature.^{29–31} Numerous inelastic electron-phonon scattering events can readily quell all shot noise across a long conductor.

We report measurements of noise in Corbino structures with inner/outer diameters of 800 μm/1200 μm, and therefore are expected to have fully suppressed shot noise from the 2D bulk. Each contact is a series combination of (gold to InAs) and then (InAs to the hybridized InAs/Ga(In)Sb interface). While we do not expect any significant barrier at the Au-InAs interface,³² there can be a band offset at the (InAs to InAs/Ga(In)Sb interface) contact when the Fermi level is in the hybridization gap. This band offset can act as a contact barrier that produces shot noise, in analogy with Schottky diodes.³³ High-frequency, broadband noise measurements

show the onset of shot noise as a function of applied bias as temperature is reduced below ~ 30 K. Analogous low-frequency noise measurements in nominally identical devices show the same trend, with zero-bias noise power consistent with Johnson-Nyquist expectations based on environmental temperature and device resistance. The detailed current-bias dependence shows only a fraction of the applied bias is generating the shot noise response. Comparison with models implies either surprisingly large Fano factors for the contacts or some shot noise generation within the 2D bulk.

Corbino structures were fabricated via a series of photolithography and wet etching steps. Devices were topped with a protective Al₂O₃ layer by atomic layer deposition and gated by a Ti/Au top gate. Figure 1a is a SEM image of one of the measured devices, Figure 1b is a schematic of the layers and contacts, and Figure 1c is a depiction of the band structure of the QWs.

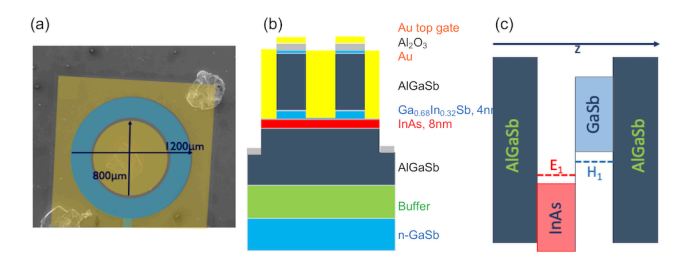


FIG. 1. (a) Colorized SEM image, yellow indicates inner and outer gold electrodes, and blue denotes the top gate; (b) Diagram of the device structure; and (c) Band structure of the QWs.

Broadband noise measurements were first performed at rf frequencies (250-600 MHz) using a lock-in technique^{34,35} described in previous reports by our group.^{36,37} A function generator applies a square-wave voltage bias across the device. Simultaneously, one lock-in amplifier measures device current response and a second monitors the change in integrated rf noise power, which is then converted via the gain-bandwidth product into average current noise power spectral density $S_I = S_I(V_{max}) - S_I(0)$. Though calibration to absolute units is difficult in this frequency

range, these measurements provide a general picture of the shot noise, free from any 1/f noise contributions.

To clarify the absolute magnitude of the current noise, we employed low frequency noise spectroscopy (0-100 kHz) based on a cross-correlation method similar to that of Hashisaka *et al.*³⁸ and by our group.³⁹ A tunable dc voltage bias is applied using a NI-DAQ6215 through strong LC filters to the sample through symmetrically placed 150 k Ω current-limiting resistors to ensure a clean voltage signal. Applying a relatively large voltage signal through the current-limiting resistors is equivalent to current-biasing the device. The sample is loaded onto a custom probe within a Janis Research Co. cryostat, with care to shield both the sample and wiring from external noise. The voltage across the sample (and its fluctuations) are individually amplified by each lownoise amplifier chain with a total gain of 10^4 and cross-correlated by a Stanford Research Systems SR785 spectrum analyzer to find the voltage noise power spectral density S_V , with amplifier noise suppressed by the cross-correlation.

Voltage noise spectra are analyzed taking into account resistive and capacitive parasitic contributions from the wiring,⁴⁰ using the relation

$$S_{V,meas} = gS_V/(1 + (2\pi f R_S C)^2)$$
 (2)

where $S_{V,meas}$ is the total measured voltage noise, g is the total amplifier gain (10⁴), $S_V = S_I R_S^2$ is the intrinsic voltage noise power spectral density from the sample, R_S is the differential resistance at the applied bias, S_I is the current noise, f is frequency and the R_SC factor denotes the decay of the measured spectrum with frequency due to the parasitic resistive and capacitive factors. The voltage noise can be converted to current noise by $S_I = S_V/R_S^2$ based on R_S found from preceding dI/dV measurements. This low-frequency technique can readily check the zero-bias noise spectrum against the expected Johnson-Nyquist noise $S_{V,JN} = 4k_BTR$, which should be white in

frequency aside from parasitic capacitance effects. At non-zero bias, the low-frequency technique is vulnerable to *1/f* noise, which results from time-varying device resistance.

Initial noise measurements were performed using the rf method. At high temperatures, thermal excitation of carriers across any hybridization gap is sufficient that the bulk 2D interface is conductive. At 100K, dI/dV measurements of the first sample showed a two-terminal zero-bias differential resistance of around 200 Ω and approximately Ohmic response. As expected, the twoterminal zero-bias resistance increased with decreasing temperature, up to 10 k Ω at 5 K. This corresponds to a square-resistance, $R_{sq} = 2\pi/\ln(r_{outer}/r_{inner})$, of roughly 155 k Ω , where r_{inner/outer} correspond to the radii of the of the inner/outer electrodes. When positively top-gated at 5 K to populate the InAs quantum well, the two-terminal resistance decreased to only 80 Ω at V_g = 0.9 V. At higher temperatures (30-100 K), lock-in detected change in noise power is essentially zero and flat with applied current bias up to 50 µA. Around 20 K, however, noise as a function of current becomes detectable, increasing with decreasing temperature, down to 5 K (Figure 2a). The critical temperature for the onset of shot noise approximately corresponds to the temperature at which conduction in the 2D bulk gaps out.⁸ Additionally, when a positive gate voltage was applied to the device, closing the bulk gap, the inferred current noise again stayed roughly zero (Figure 2b).

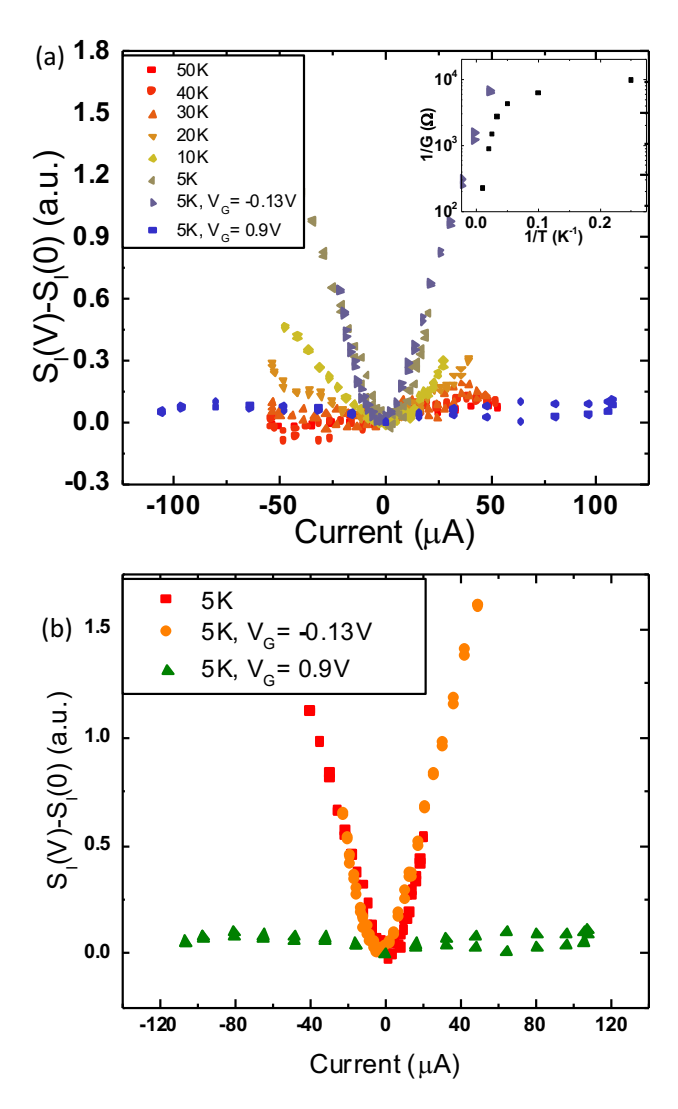


FIG. 2. Integrated current noise in rf bandwidth \sim 250-600 MHz as a function of temperature (a) and gate bias (b). (Inset) Resistance versus temperature. Shot noise is essentially fully suppressed at high temperatures and positive gate voltages, when the bulk is conductive. The shot noise contribution begins to turn on with increasing current at around 20 K, as bulk transport gaps out, and continues to grow with decreasing temperature.

Voltage noise was measured in additional devices at low frequencies. At zero bias, the voltage noise was consistent with the Johnson-Nyquist expectations for the measured resistance. Again, the noise remained roughly constant with applied current at higher temperatures, but started to increase with increasing current below ~20 K (Figure 3a), consistent with the onset of some shot noise contribution. The magnitude of the bias-dependent noise, however, was consistently much smaller and had a broader curvature around zero bias than expected if one naively applied

Equation 1 for a given conductance and temperature, assuming a Fano factor of 1 and that all the voltage bias contributes to the argument of the coth term (Figure 3b).

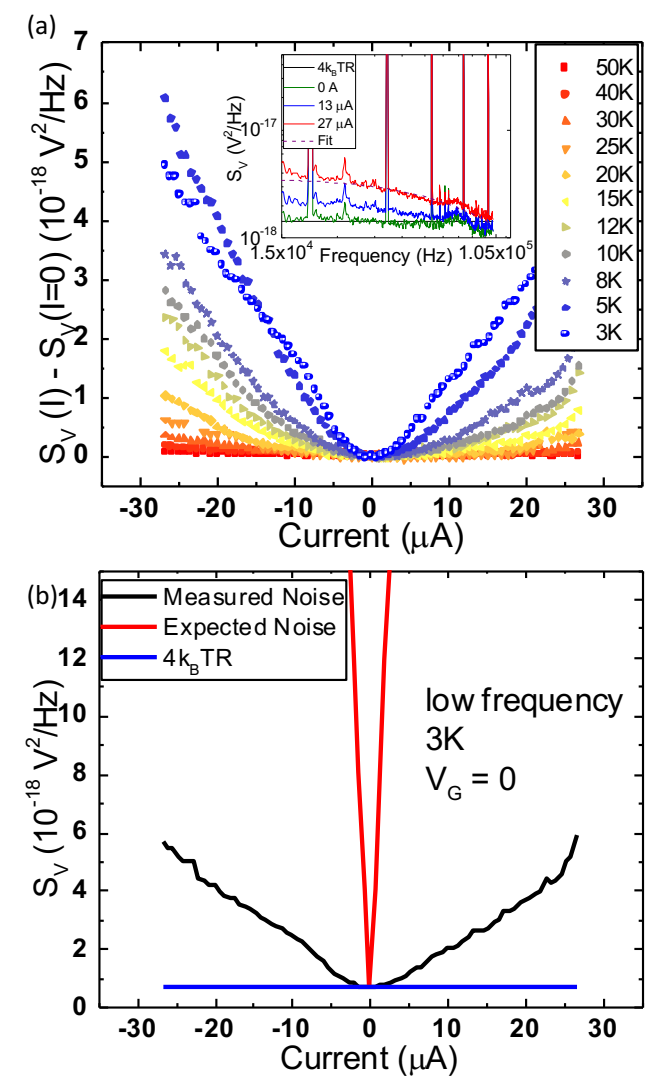


FIG. 3. (a) Voltage noise minus zero-bias noise as a function of temperature. Noise is relatively flat above 20 K but then increases with decreasing temperature. (Inset) Example spectra at 8 K at 0, 13, and 27μA. Spikes are from environmental pickup and do not affect the analysis. Black line indicates Johnson-Nyquist, and purple dotted line indicates fit to Equation 2, with $S_V = 3.41 \times 10^{-18} \text{ V}^2/\text{Hz}$ and $2\pi R_S C = 1.1 \times 10^{-5} \text{ s}$. (b) Compared to Equation 1, assuming all of the applied bias is contributing to the shot noise, the magnitude of the noise at 3 K is much smaller than expected and the curvature about zero bias is much broader.

Particularly motivated by the breadth of the curvature of the noise near zero bias, we attempt to model the measured noise through the equivalent circuit shown in Figure 4a, namely

three series resistors: two contact resistances (assumed for simplicity to be identical) and a bulk resistance representing the 2D Corbino bulk contribution. We assume the band offset at each InAs-InAs/Ga(In)Sb contact is the dominant source of contact resistance and can act as a barrier that produces shot noise. In the simplest situation, we assume the bulk resistance, R_b , and the contact resistances, R_c , are Ohmic, with the total resistance $R = 2R_c + R_b$. In general, for a non-Ohmic device, the resistances should be differential resistances found self-consistently under biasing conditions such that the total voltage across the three resistors in series is the applied dc bias across the device, $V_{dev} = R \times V_{tot}/(R + 300 \text{ k}\Omega)$, where R is the two-terminal device resistance, V_{tot} is the total dc voltage applied by the DAQ, and 300 k Ω accounts for the series resistances. In the temperature range studied here, the device is still relatively Ohmic, and thus it is unlikely to be in the limit of Poole-Frenkel hopping transport. As temperature approaches zero and the system reaches a limit where all carriers are frozen out, it would be necessary to reevaluate the primary charge transport mechanism. In this simplified model, however, the bulk is considered diffusive and large compared to inelastic electron-phonon scattering scales, and therefore should contribute only to the Johnson-Nyquist thermal noise, with all non-equilibrium shot noise arising at the contacts. Factoring in finite temperature contributions, including the thermal noise and that the voltage dropped across each contact is $IR_c=V_c$, the total voltage noise in the Corbino should be⁴¹

$$S_V = 4FeIR_c^2 \coth(eV_c/2k_BT) + 4k_BT(R_b + 2(1 - F)R_c).$$
 (3)

Within this model, at high bias $(eV_c \gg 2k_BT)$, the $S_V(I)$ data can be fit to a line, with slope $m = 4eFR_c^2$ and intercept $b = 4k_BT(R_b + 2(I-F)R_c) = 4k_BT(R - 2FR_c)$. This is used to derive values for the Fano factor and contact resistance. Figure 4b compares the results of the model in Equation 3 to the voltage noise measured at 3 K in the low frequency setup. This model provides a natural explanation to the voltage scale of the rounding near zero bias, with only a fraction of the applied

voltage actually dropping across each shot-noise-producing contact.

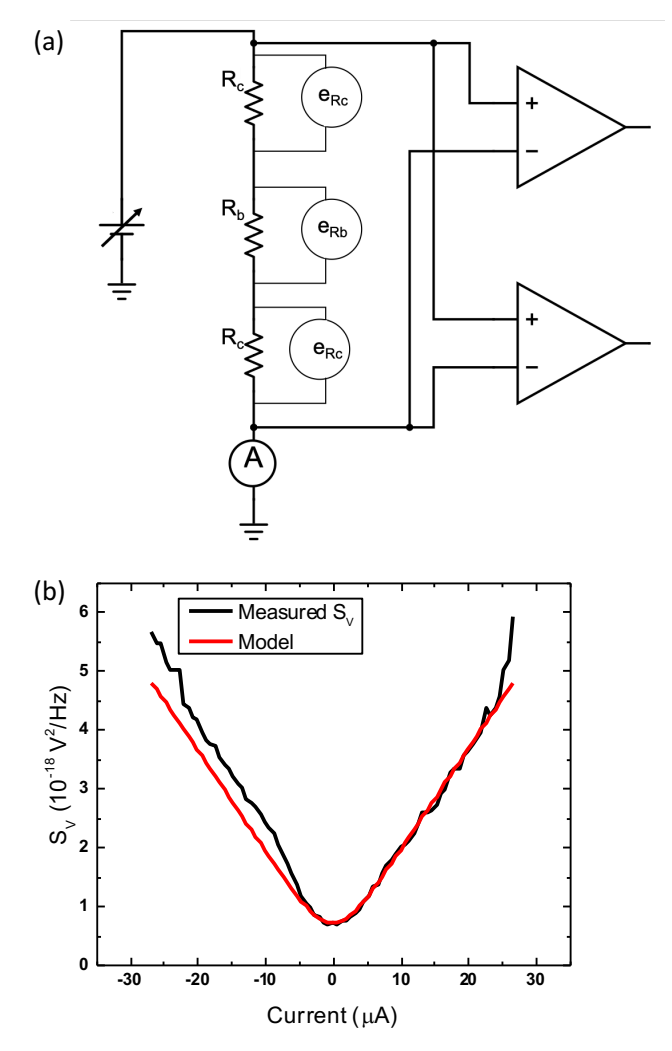


FIG. 4. Equivalent circuit (a) and comparison to data (b) of the model described by Equation 3, with $R = 4.34 \text{ k}\Omega$, $F = 5.76 \pm 0.2$, and $R_c = 217 \pm 6 \Omega$. Both contact resistances and the resistance of the bulk contribute to the Johnson-Nyquist noise, but any contribution to the shot noise from the bulk is suppressed, leaving only contributions from the two contacts. Voltage division between contacts and bulk accounts for the low bias curvature scale, but implies surprisingly large Fano factors for the contacts.

Figure 5 shows the Fano factors and contact resistances derived from linear fitting of high bias data from an example device measured at low frequency. Negative and positive current data were fitted separately due to the asymmetric nature of the $S_V(I)$ curves (present even when the I-V response is Ohmic). We attribute this asymmetry to differences in the inner and outer contacts

arising during the etching processes of the fabrication. From the high bias linear fits, we find that contact resistance is generally small, on the order of 10% or less of the total device resistance. While the error bars are obtained from reasonable goodness of fits for each temperature individually, the degree of scatter among all the data points suggests the systematic uncertainties are comparable to or greater than any trend with temperature. At higher temperatures, the Fermi distribution of carriers in the metal is broadened, and the bulk of the 2D interface (where the Ga(In)Sb hole and InAs electron quantum well states hybridize to form the bulk gap) should have greater thermal activation of carriers between the lower and upper hybridized bands. Disorder also leads to a spatially varying energy landscape within the 2D bulk, when the Fermi level lies in the gap, which localizes residual charge carriers as temperature goes to zero. 42 Therefore, naively one would expect higher free carrier densities at higher temperatures would yield lower contact resistances. The contact resistances inferred from our model do not appear to fit this trend, but we have excluded any disorder effects and have not attempted to incorporate the Fermi level pinning or charge transfer at the contacts, which could influence the effective height and width of any barrier at the InAs to InAs/Ga(In)Sb interface.

The Fano factor inferred from the model tends to increase with decreasing temperature, as expected for a Schottky contact. The inferred values of F, however, are greater than 1, up to over 10 in some cases, indicating either some contribution to the shot noise from the bulk (not captured in the model), or a noise-enhancing process at the contacts. In considering possible contributions from the bulk, as thermal activation of carriers over the gap in the 2D bulk is suppressed at lower temperatures, disorder can lead to both puddles of charge⁴³ and residual charge⁴² bound in localized states. Tunneling through this irregular potential landscape could contribute to the noise. The 2D bulk is essentially in the macroscopic limit, however, and if the system were in the limit

of many puddles or localized states, the net shot noise would be fully suppressed, similar to the 1/N reduction of shot noise in N identical tunnel junctions in series.⁴¹ This leads us to believe the shot noise arises at a small number of interfaces.

One possibility for enhanced Fano factors at low temperatures is positive feedback between tunneling electrons and space charge near one of the contacts. This mechanism for enhanced noise was first put forth by Reklaitis and Reggiani⁴⁴ who modelled a single barrier heterostructure of GaAs/Al_{0.25}Ga_{0.75}As. They found Fano factors up to 7 because of positive feedback between tunneling probability and a build-up of space charge near the barrier. While difficult to precisely model our system for space charge effects, we believe this could be one reasonable explanation for the large Fano factors derived from the data. The tendency for the Fano factor to increase with decreasing temperature, as the bulk becomes more gapped, would be consistent with an increase in space charge near the contacts.

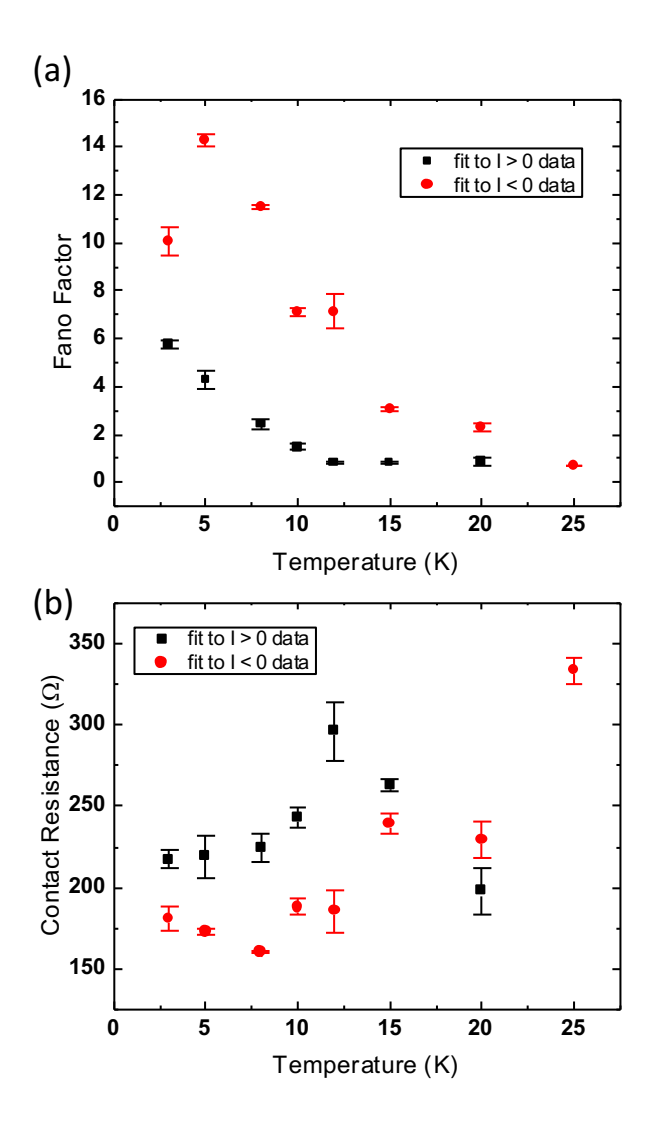


FIG. 5. Fano factors (a) and contact resistances (b) derived from linear fits of high bias $S_V(I)$ data taken at low frequency for the model of Eq. (3). Error bars calculated based on standard deviations of slope and intercept of fit. Contact resistance is generally small relative to the total device resistance. Fano factors tend to increase with decreasing temperature.

In summary, we have performed low frequency and rf noise spectroscopy measurements on InAs/Ga(In)Sb Corbino structures to gain a better understanding of the transport properties and shot noise characteristics of the 2D bulk and the contacts. At higher temperatures, voltage noise remains relatively current independent about the thermal noise level. As temperature is decreased and the 2D bulk is expected to gap out, however, shot noise becomes detectable. Naively, treating the device as a single noise source, the magnitude of the shot noise appears much smaller than 2eI

and the curvature of the noise about zero bias is too broad for the given conductance and temperature of the device. We have found the noise fits well to a model in which the applied bias is dropped over two contacts and the bulk, wherein only the voltage dropped over the contact resistances contributes to the shot noise, but all three contribute to the thermal noise. Assuming voltage division between bulk and contacts reproduces the low bias noise dependence with reasonably small contact resistances, but at the cost of anomalously large Fano factors. One candidate explanation for the enhanced Fano factors is positive feedback between the tunneling probability and space charge at the interface of the bulk and contacts. These findings show that contacts to bulk 2DTI interfaces can have nontrivial noise response.

Acknowledgements

We acknowledge G. Sullivan for providing the structures grown by molecular beam epitaxy. TL and RRD acknowledge NSF Grant No. DMR-1508644 for financial support. DN and LAS acknowledge NSF Grant No. DMR-1704264 for financial support, and Panpan Zhou, Liyang Chen, Xuanhan Zhao, and Yue Liu for helpful conversations. Some measurement hardware was purchased with the support of DOE BES award DE-FG02-06ER46337.

- ¹ M.Z. Hasan and C.L. Kane, Rev. Mod. Phys. **82**, 3045 (2010).
- ² C.L. Kane and E.J. Mele, Phys. Rev. Lett. **95**, 146802 (2005).
- ³ B.A. Bernevig, T.L. Hughes, and S.-C. Zhang, Science (80-.). **314**, 1757 (2006).
- ⁴ X.L. Qi and S.C. Zhang, Rev. Mod. Phys. **83**, 1057 (2011).
- ⁵ M. König, S. Wiedmann, C. Brüne, A. Roth, H. Buhmann, L.W. Molenkamp, X.-L. Qi, and S.-C. Zhang, Science (80-.). **318**, 766 (2007).
- ⁶ L. Du, I. Knez, G. Sullivan, and R.-R. Du, Phys. Rev. Lett. **114**, 096802 (2015).
- ⁷ F. Couëdo, H. Irie, K. Suzuki, K. Onomitsu, and K. Muraki, Phys. Rev. B **94**, 035301 (2016).
- ⁸ L. Du, T. Li, W. Lou, X. Wu, X. Liu, Z. Han, C. Zhang, G. Sullivan, A. Ikhlassi, K. Chang, and R.-R. Du, Phys. Rev. Lett. **119**, 056803 (2017).
- ⁹ M.J. Yang, C.H. Yang, B.R. Bennett, and B. V. Shanabrook, Phys. Rev. Lett. **78**, 4613 (1997).
- ¹⁰ C. Liu, T.L. Hughes, X.-L. Qi, K. Wang, and S.-C. Zhang, Phys. Rev. Lett. **100**, 236601 (2008).
- ¹¹ I. Knez, R.R. Du, and G. Sullivan, Phys. Rev. B **81**, 201301 (R) (2010).
- ¹² I. Knez, R.-R. Du, and G. Sullivan, Phys. Rev. Lett. **107**, 136603 (2011).
- ¹³ W. Pan, J.F. Klem, J.K. Kim, M. Thalakulam, M.J. Cich, and S.K. Lyo, Appl. Phys. Lett. **102**, 033504 (2013).
- ¹⁴ K. Suzuki, Y. Harada, K. Onomitsu, and K. Muraki, Phys. Rev. B Condens. Matter Mater. Phys. **91**, 245309 (2015).
- ¹⁵ S. Mueller, A.N. Pal, M. Karalic, T. Tschirky, C. Charpentier, W. Wegscheider, K. Ensslin, and T. Ihn, Phys. Rev. B **92**, 081303 (2015).
- ¹⁶ F. Qu, A.J.A. Beukman, S. Nadj-perge, M. Wimmer, B. Nguyen, W. Yi, J. Thorp, M.

- Sokolich, A.A. Kiselev, M.J. Manfra, C.M. Marcus, and L.P. Kouwenhoven, Phys. Rev. Lett. **115**, 036803 (2015).
- ¹⁷ F. Nichele, H.J. Suominen, M. Kjaergaard, C.M. Marcus, E. Sajadi, J.A. Folk, F. Qu, A.J.A. Beukman, F.K. de Vries, J. van Veen, S. Nadj-Perge, L.P. Kouwenhoven, B.-M. Nguyen, A.A. Kiselev, W. Yi, M. Sokolich, M.J. Manfra, E.M. Spanton, and K.A. Moler, New J. Phys. **18**, 083005 (2016).
- ¹⁸ B.-M. Nguyen, A.A. Kiselev, R. Noah, W. Yi, F. Qu, A.J.A. Beukman, F.K. De Vries, J. Van Veen, S. Nadj-perge, L.P. Kouwenhoven, M. Kjaergaard, H.J. Suominen, F. Nichele, C.M. Marcus, M.J. Manfra, and M. Sokolich, Phys. Rev. Lett. 117, 077701 (2016).
- ¹⁹ T.L. Schmidt, Phys. Rev. Lett. **107**, 096602 (2011).
- ²⁰ B. Rizzo, L. Arrachea, and M. Moskalets, Phys. Rev. B **88**, 155433 (2013).
- ²¹ J.M. Edge, J. Li, P. Delplace, and M. Buttiker, Phys. Rev. Lett. **110**, 246601 (2013).
- ²² F. Dolcini, Physical **92**, 155421 (2015).
- ²³ A. Del Maestro, Phys. Rev. B **87**, 165440 (2013).
- ²⁴ P.P. Aseev and K.E. Nagaev, Phys. Rev. B **94**, 045425 (2016).
- 25 J.I. Väyrynen and L.I. Glazman, Phys. Rev. Lett. $\boldsymbol{118},\,106802$ (2017).
- ²⁶ K.E. Nagaev, S. V. Remizov, and D.S. Shapiro, J. Exp. Theor. Phys. Lett. **108**, 664 (2018).
- ²⁷ P.D. Kurilovich, V.D. Kurilovich, I.S. Burmistrov, Y. Gefen, and M. Goldstein, arxiv:1903.03965 (2019).
- ²⁸ Y.M. Blanter and M. Buttiker, Phys. Rep. **336**, 1 (2000).
- ²⁹ C.W.J. Beenakker and M. Buttiker, Phys. Rev. B **46**, 1889 (1992).
- ³⁰ A.H. Steinbach, J.M. Martinis, and M.H. Devoret, Phys. Rev. Lett. **76**, 3806 (1996).
- ³¹ A. Shimizu and M. Ueda, Phys. Rev. Lett. **69**, 1403 (1992).

- ³² S. Bhargava, H.-R. Blank, V. Narayanamurti, and H. Kroemer, Appl. Phys. Lett. **70**, 759 (1997).
- ³³ A.M. Cowley and R.A. Zettler, IEEE Trans. Electron Devices **15**, 761 (1968).
- ³⁴ M. Reznikov, M. Heiblum, H. Shtrikman, and D. Mahalu, Phys. Rev. Lett. **75**, 3340 (1995).
- ³⁵ S.E.S. Andresen, F. Wu, R. Danneau, D. Gunnarsson, and P.J. Hakonen, J. Appl. Phys. **104**, 033715 (2008).
- ³⁶ L.A. Stevens, P. Zolotavin, R. Chen, and D. Natelson, J. Phys. Condens. Matter **28**, 495303 (2016).
- ³⁷ P.J. Wheeler, J.N. Russom, K. Evans, N.S. King, and D. Natelson, ACS Nano Lett. **10**, 1287 (2010).
- ³⁸ M. Hashisaka, T. Ota, M. Yamagishi, T. Fujisawa, and K. Muraki, Rev. Sci. Instrum. **85**, 054704 (2014).
- ³⁹ P. Zhou, L. Chen, Y. Liu, I. Sochnikov, A.T. Bollinger, M.-G. Han, Y. Zhu, X. He, I. Bozovic, and D. Natelson, Nature in press (2019).
- ⁴⁰ C. Sabater, M. Kumar, S. Stahl, B. Crama, and J.M. van Ruitenbeek, Rev. Sci. Instrum. **88**, 093903 (2017).
- ⁴¹ R. Landauer, Phys. B **227**, 156 (1996).
- ⁴² Y. Naveh and B. Laikhtman, Europhys. Lett. **55**, 545 (2001).
- ⁴³ J.I. Väyrynen, M. Goldstein, and L.I. Glazman, Phys. Rev. Lett. **110**, 216402 (2013).
- ⁴⁴ A. Reklaitis and L. Reggiani, Phys. Rev. B **62**, 16773 (2000).